






Machine learning based crystal collimator alignment optimization

Gianmarco Ricci ^{*}, Marco D'Andrea , Mario Di Castro, Eloise Matheson, Daniele Mirarchi ,
Andrea Mostacci ^{*} and Stefano Redaelli
CERN, CH-1211 Geneva 23, Switzerland

 (Received 10 January 2024; accepted 12 August 2024; published 24 September 2024)

In the CERN Large Hadron Collider (LHC), bent crystals are used to efficiently deflect beam halo particles toward secondary collimators used as absorbers. In this crystal collimation scheme, a crystal with a length of a few millimeters can produce a deflection equivalent to a magnetic field of hundreds of Tesla at LHC top energies, improving the cleaning performance of the machine. However, crystals must be in optimal alignment with respect to the circulating beam to maximize the efficiency of the channeling process. A newly developed machine learning model automatically classifies the channeling condition of crystals using beam loss monitor signals during slow rotation of the crystal. This advancement represents a crucial step toward refining the process of identifying the optimal channeling orientation. The algorithm has been tested for the first time in operation with Pb ion beams at the record energy of 6.8 Z TeV demonstrating its reliability.

DOI: [10.1103/PhysRevAccelBeams.27.093001](https://doi.org/10.1103/PhysRevAccelBeams.27.093001)

I. INTRODUCTION

At the European Organization for Nuclear Research (CERN) Large Hadron Collider (LHC) [1], proton and heavy ion beams are brought into collision to conduct high-energy physics experiments. Due to several processes, some particles inevitably stray from the central beam (forming the so-called “halo”), resulting in unavoidable losses as the beam circulates in the accelerator. Therefore, a robust collimation system is needed to intercept particles that deviate from the desired trajectory and safely dispose of these losses [2]. CERN is currently engaged in a major upgrade project of the LHC, known as the High-Luminosity LHC (HL-LHC) [3], with the goal to achieve an integrated luminosity of 250 fb^{-1} per year [4]. Enhancements to the collimation system are essential, particularly during heavy ion operations, to address the heightened operational challenges posed by the Hi-Lumi LHC project [5].

One of the upgrades will rely on the use of crystal collimation. The concept utilizes the highly ordered atomic structure of crystals to channel charged particles into potential wells formed by adjacent crystal planes [6]. Particles that deviate from the intended trajectory of the beam are forced to follow the curvature of the bent crystal [7],

^{*}Also at Università degli Studi di Roma “La Sapienza,” Piazzale Aldo Moro 5, 00185 Rome, Italy.

Published by the American Physical Society under the terms of the *Creative Commons Attribution 4.0 International license*. Further distribution of this work must maintain attribution to the author(s) and the published article’s title, journal citation, and DOI.

and crystals as short as 4 mm in length with $50 \text{ } \mu\text{rad}$ bending angle can generate equivalent bending fields of 300 Tesla at LHC top energy, directing halo particles toward specific locations where secondary collimators are used as absorbers [8] (see Fig. 1). This technique has clear implications for beam collimation. The upgrade was tested during the LHC Run 3 operations (2022 to 2025), to deliver higher ion luminosity to the experiments.

Achieving optimal performance requires angular alignment with μrad precision of the crystal with respect to the beam envelope, a highly challenging task. Previously, the angular alignment of the crystal with the circulating beam was achieved “manually,” using visual human feedback to determine when the channeling signature is found based on signals from beam loss monitors during crystal rotational scans. However, this manual alignment procedure is time-consuming, taking hours of valuable machine time away from physics experiments. To address this challenge, the aim of this work is to enhance the alignment process by automating the classification of channeling signatures

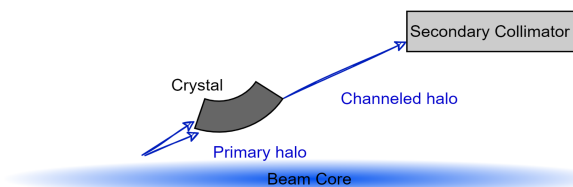


FIG. 1. Illustrative view of the crystal channeling primary halo particles onto secondary collimator. The optimal channeling orientation can be found by observing losses on the crystal and secondary collimator.

using deep learning. This work can improve the efficiency and accuracy of identifying the optimal channeling orientation in an automated way compared to the manual approach.

This paper presents a deep learning framework based on a 1D-convolutional neural networks (CNN) to optimize the search for the crystalline planes. The problem under study is a time-series classification, therefore, this falls under the category of supervised learning [9]. Additionally, in this work, an algorithm to deploy the developed machine learning model has been engineered.

II. CONVENTIONAL AND CRYSTAL COLLIMATORS SCHEMES

The current LHC collimation system is composed of 110 collimators, each with two movable blocks referred to as “jaws.” They are placed symmetrically around the circulating beams in a multistage hierarchy that ensures an optimal cleaning performance. In the LHC a three-stage hierarchy is used. This consists of primary collimators (TCP), which are closest to the beam and intercept the primary halo particles, secondary collimators (TCSG), that intercept secondary halo particles and the hadronic shower and finally absorber collimators (TCLA), made of tungsten alloy, that absorb the hadronic showers developed in the first two collimation stages [3]. The simplified structure of the collimation system is depicted in Fig. 2, while a more exhaustive description of the collimation system can be found in [2,10,11].

The multistage collimation system used in the LHC is less efficient for ion beams compared to protons. This is because when ions interact with conventional collimator materials, nuclear fragmentation processes occur. These processes generate ion fragments with different magnetic rigidities but fail to provide enough transverse kicks to steer these fragments toward the secondary collimators. As a result, these fragments pass through the “betatron” collimation system area (responsible for safely handling transverse beam losses). Consequently, due to a local rise in temperature, there is an elevated risk of quenching in the superconductive magnets [12,13]. Given that the losses generated by high-intensity ion beams were already approaching the quench limits of the superconducting

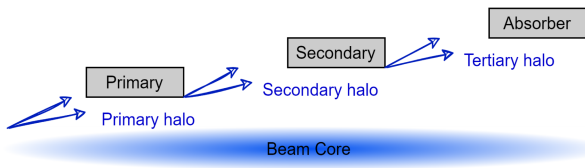


FIG. 2. Illustrative and simplified view of the three stage collimation system. Primary collimators intercept primary halo particles, secondary collimators intercept secondary halo particles, and absorber collimator absorbs the hadronic showers developed in the first two collimation stages.

magnets during Run 2 (operations from 2015 to 2018) [14], to achieve the goals set by the Hi-Lumi LHC project an upgrade of the present collimation system is needed.

As noted in Ref. [5], the LHC upgrade also involves the adoption of crystal collimation. This method utilizes bent crystals to guide halo particles, channeling them toward a single absorber in either the vertical or horizontal plane. The principle of crystal planar channeling is leveraged to accomplish this task efficiently. Ideally, a single crystal per plane suffices, paired with an absorber designed to capture the channeled particles.

Crystal collimation provides two primary benefits. First, the likelihood of inelastic interactions within a crystal collimator is significantly lower than that for a standard collimator. This is because channeled particles travel through the relatively empty space between lattice planes, resulting in fewer losses caused by interactions with the atomic nuclei; second, crystal collimation presents a notable decrease in the impedance budget within particle accelerators. Impedance denotes the collective effect of the electromagnetic interactions between the circulating particle beam and the surrounding accelerator structure. In contrast to conventional primary collimators, crystal collimators feature a considerably more condensed structure, thereby driving down impedance levels. Additionally, during operations with crystals, the secondary collimator used as an absorber is more distant from the circulating beam, further mitigating impedance effects [15]. These advantages make crystal collimation an attractive option for beam collimation in high-energy particle colliders [15,16].

The angular orientation of the crystal must be finely adjusted with a precision below $1\mu\text{rad}$ to ensure that the channeling conditions are respected. This is due to the “critical angle”—the maximum angle of incidence (with respect to the crystalline planes) at which particles can be channeled by the crystal lattice. It represents the threshold angle beyond which the channeling effect becomes ineffective, and particles are more likely to undergo other coherent phenomena rather than being channeled along a specific crystal plane. For example, as reported in [17], at 7 TeV the critical angle is $2.4\mu\text{rad}$. One extra challenge that occurs during the alignment of a crystal collimator is the existence of additional symmetries referred to as skew planes (SK), which appear diagonally in relation to the planes utilized for channeling. SK can trap charged particles, but with a lower efficiency (because of the lower potential well they can generate) and with a lower deflection angle compared to channeling, reducing the channeling efficiency of the crystal collimation concept [18]. Therefore, it is crucial to avoid these planes when aligning the device with the circulating beam.

III. ANGULAR SCAN

The optimal channeling orientation can be identified using beam loss monitors (BLMs) [19,20] positioned

adjacent to both the crystal and the secondary collimator. They are designed to detect beam losses in particle accelerators by measuring the ionization produced when beam particles interact with the surrounding material at specific locations along the beamline. This ionization process detected by the BLM generates a signal that can be measured in units of Gy/s.

The crystals are installed on precise goniometers, which include both a linear and rotational stage. The linear stage enables the crystal to be inserted in the beam line until it makes contact with the beam halo, while the rotational stage allows for accurate angular positioning to locate the channeling orientation. The goniometers provide exceptional angular resolution, with a precision level below $0.1 \mu\text{rad}$ [21]. The main steps to find the channeling orientation of a crystal collimator are movement of the crystal collimator toward the beam until it touches the beam halo, followed by slow rotation of the crystal until the channeling signature is observed [18].

During this procedure, called *angular scan*, the BLM signals at the location of the crystal and of the secondary collimator that intercepts the deflected beam are monitored. As seen in Fig. 3, the channeling signature is composed of three main patterns: (i) amorphous plateaus, where the orientation is so far away from optimal channeling that the crystal behaves like any amorphous scatterer; (ii) channeling well, minimum in the loss pattern observed at the crystal location due to reduced inelastic interaction rate and increase of losses in correspondence of the secondary collimator that intercepts the channelled particles (Fig. 1); and (iii) volume reflection plateau, where particles bounce off of the crystalline planes instead of being channelled [22]. It is important to note that to better observe the characteristic signature of channeling from the BLM signal, white noise is introduced into the beam using the active transverse damper [23]. This increases the diffusion speed of the halo, causing intentional but controlled beam losses during the scan. Nevertheless considering the angular range of the goniometer of 20 mrad and the average scan

step size of $1 \mu\text{rad/s}$, finding the channeling orientation is a nontrivial operation that can take hours of machine time.

The objective of this work is to tackle this task improving the alignment procedure through automatic categorization of channeling patterns using deep learning techniques.

IV. DATASET OVERVIEW: COMPOSITION AND CHARACTERISTICS

The quality and amount of data used to train a machine learning model can greatly affect its performance and generalization ability, and therefore, careful data collection has been performed to ensure the reliability of the results. Hence, in this study, the dataset employed for training and evaluating the machine learning model comprises 1689 sets labeled from hundreds of angular scans by collimation experts. To enhance the dataset variability and its capacity to generalize effectively across diverse scenarios, a technique known as data augmentation was implemented. This process involved the integration of signals derived from multiple beam loss monitors strategically situated around the ring during angular scans. The incorporation of these signals facilitated the development of detection patterns that are compatible with the problem under investigation. The scans were performed on both beams in the horizontal and vertical planes at different beam energies. These sets consist of 1 Hz BLM signals gathered during machine development studies with proton and Pb ion beams from 2015 to 2022. Each set is comprised of two time-series signals: one registered in correspondence of the crystal and one in correspondence of the secondary collimator.

The BLM signals have been distributed into a main dataset used for training and a validation set (which corresponds to roughly 20% of the main dataset) used for testing the model on randomly chosen and unseen data. Both have been divided in three classes. Table I presents a detailed overview of the dataset composition utilized in the study. This table illustrates the distribution of signal counts across various classes within both the main dataset and the validation set.

A signal belonging to the channeling well class (Fig. 3) is a BLM signal that exhibits the channeling signature described in Sec. III. In contrast, a signal categorized as no channeling (Fig. 4) lacks a discernible channeling pattern, while a signal classified as “partial well” (or “anomalous

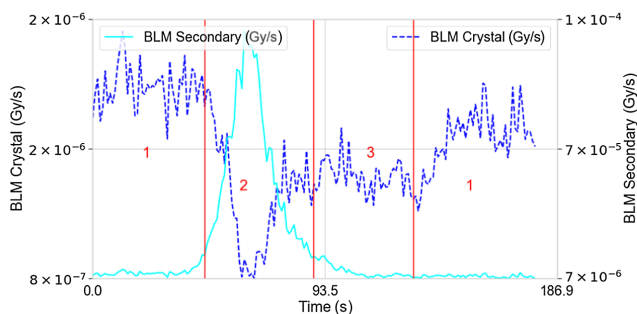


FIG. 3. BLM signal as a function of time while crystal is rotating identified as a “channeling well” (dark blue line). BLM signal as a function of time observed in correspondence of the secondary collimator, while crystal is rotating (light blue line).

TABLE I. Composition of datasets.

Class	Dataset	Signal counts
Channeling well	Main dataset	530
	Validation set	125
No channeling	Main dataset	354
	Validation set	61
Partial well	Main dataset	509
	Validation set	110

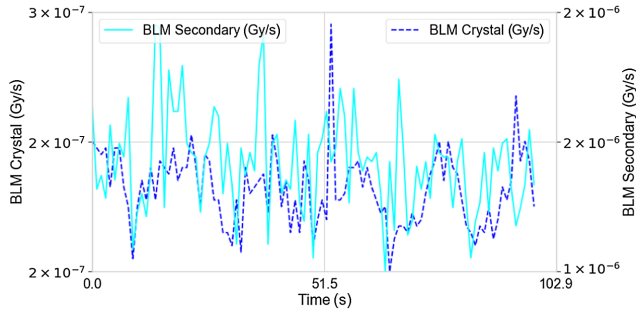


FIG. 4. BLM signals registered in correspondence of crystal and secondary collimators during angular scan identified as “no channeling”.

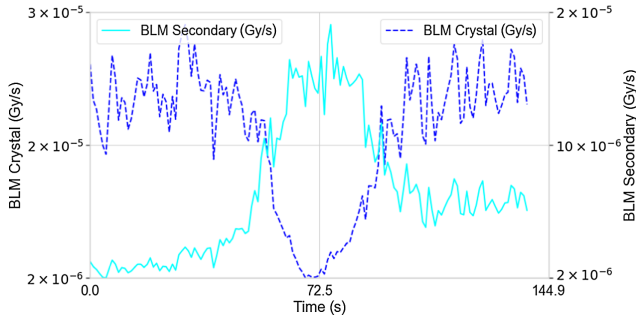


FIG. 5. BLM signals registered in correspondence of crystal and secondary collimators during angular scan identified as partial well.

channeling”) can be seen in Fig. 5 and it displays the channeling pattern but not the volume reflection pattern. One of the objectives of this work was to prevent the incorrect identification of a partial well and differentiate it from a channeling well, as a partial well may lead to decreased particle deflection, resulting in reduced efficiency.

V. CONVOLUTIONAL NEURAL NETWORK MODEL DESIGN

According to [24], 1D-convolutional neural networks have recently been proposed and immediately achieved state-of-the-art performance levels in several applications, such as personalized biomedical data classification and early diagnosis, structural health monitoring, anomaly detection and identification in power electronics, and electrical motor fault detection. Other endeavors at various facilities, focusing on distinct machine subsystems and employing diverse methodologies, demonstrate the encouraging prospects of machine learning [25,26]. An additional significant benefit is the feasibility of implementing real-time and cost-effective hardware due to the simple and compact nature of 1D CNNs, which solely perform 1D convolutions. Therefore, the chosen machine learning model trained to classify channeling conditions of a crystal

collimator is a feature-less 1D CNN. This is a type of neural network architecture that does not require manual feature engineering, as it automatically extracts relevant features from the input data.

In signal classification, 1D CNNs are commonly used to classify time-series data by learning the underlying patterns and relationships in the data. This approach can be particularly effective when working with unprocessed BLM data, as the model can learn to recognize meaningful features in the data without the need for preprocessing or feature extraction. The model engineered in this work has been developed using the deep learning library KERAS [27] with a TensorFlow [28] backend.

Before feeding the data into the first CNN layer, a Z-score normalization at each signal is applied such that they have the properties of a standard normal distribution with mean $\mu = 0$ and standard deviation $\sigma = 1$ [29]. Standard scores of the samples x are calculated as follows:

$$z = \frac{x - \mu}{\sigma}. \quad (1)$$

The detailed network design of the 1D CNN shown in Table II presents the architecture layers and corresponding output shapes. The first column in this table represents the sequence of layers composing the architecture, while the “output shape” column encapsulates the batch size (number of training examples utilized in one iteration of the training process), the length of the signal that is being processed by the neural network, and channel dimensions of the data produced by the layers. The dimensions are presented in a tuple format, where each element in the tuple corresponds to a specific dimension. The placeholders “batch size” and “signal length” in the tuple signify that these dimensions vary during the training process based on the characteristics of the dataset being used.

The developed model consists of two 1D convolutional layers followed by batch normalization layers, rectified linear unit activation functions, and dropout layers, with respective frequency rates of 0.75 and 0.6, adopted to reduce overfitting. In a classification problem, the output of

TABLE II. Network architecture layers and output shapes.

Layer(s)	Output shape
Conv1D	(Batch size, signal length, 256)
Batch normalization	(Batch size, signal length, 256)
ReLU	(Batch size, signal length, 256)
Dropout	(Batch size, signal length, 256)
Conv1D	(Batch size, signal length, 160)
Batch normalization	(Batch size, signal length, 160)
ReLU	(Batch size, signal length, 160)
Dropout	(Batch size, signal length, 160)
Global average pooling	(Batch size, 160)
Dense	(Batch size, 3)

a neural network commonly comprises a vector of scores. Each element within this vector indicates the level of confidence exhibited by the network regarding the input's association with a specific class. To achieve this, the CNN architecture aforementioned is closed by a 1D global average pooling layer and a dense layer with three output nodes, accompanied by a softmax activation function. The softmax function normalizes the vector of scores ensuring that their summation results in unity. Consequently, the network's output can be interpreted as a probability distributions. In other words, the choice of the activation function allows the output of three different probabilities, precisely the probabilities that the time series analyzed shows a pattern compatible with Figs. 3, 4, or 5.

To achieve optimal performance on the given classification task, two key techniques have been used: early stopping [30] and random search for hyperparameter tuning [31]. The early stopping technique was implemented to monitor the validation performance of the model during the training process and halt the training when the validation performance plateaued, thereby preventing overfitting. Additionally, the model underwent fine tuning. In particular, 50 sets of hyperparameters from a predefined search space have been sampled, and the CNN has been trained for each set of hyperparameters. The performances have been evaluated on a held-out validation set, and the hyperparameters that resulted in the best performance have been selected.

VI. MODEL EVALUATION

The performance of the model has been evaluated with the use of the precision metric:

$$\text{Precision} = \frac{\text{TP}}{\text{TP} + \text{FP}}, \quad (2)$$

where true positives (TP) indicate the number of signals of the class that are correctly predicted by the algorithm, and false positives (FP) indicate the number of signals not belonging to the class that are mistakenly classified.

The 1D CNN model achieved an average precision of 93% on the unseen validation set BLM signals with proton and ion beams, which served as a benchmark for the conducted experiment. The confusion matrix depicted in Fig. 6 offers a comprehensive breakdown of the model's performance, facilitating precision assessment. In instances where a CNN incorrectly labels a channeling well as a partial well, it may necessitate rescanning the crystal within the previously examined range, at a reduced rotational speed to enhance the patterns detection in the BLMs signals. Despite this, such results are promising, indicating the reliability of convolutional neural networks in identifying main planar channeling, showcasing their potential for practical applications.

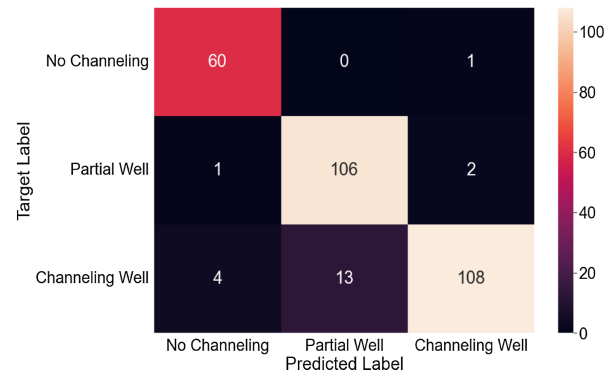


FIG. 6. Confusion matrix obtained by classifying validation set signals.

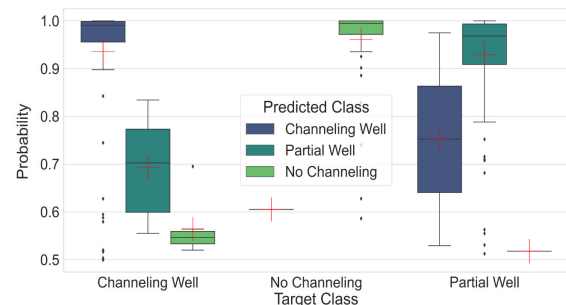


FIG. 7. Classification probabilities distributions of validation set signals with respect to the target classes. The average classification probability is indicated by a red cross within the boxplot.

Figure 7 depicts the predicted probability distributions of the CNN applied to the validation set signals, regarding the three targeted classes. These outcomes reveal that the model presents high levels of confidence in its classification performance on previously unseen validation data.

VII. PROPOSED IMPLEMENTATION APPROACH

In this section, a framework to deploy the developed machine learning model into operational settings is presented. The machine learning model has been implemented into a software application [32] designed to streamline and consolidate all major operational requirements for crystal collimation, one of which is the identification of the correct channeling orientation. The application enables the control of the rotational stage of the goniometer, and the online classification of beam loss monitors signals. In particular, the tool allows the definitions of the settings of the angular scan, such as start scan position, stop scan position, and scan speed. During the rotation of the crystal, the BLM signals of fixed length are fed into the machine learning model. The classification window (W) is determined with the following formula:

$$W[s] = 4 \frac{\theta(\mu\text{rad})}{\dot{\theta}(\mu\text{rad/s})}, \quad (3)$$

where θ is the crystal bending angle (defined as $\theta = \frac{l}{R}$, where l is the crystal length in the beam direction and R its bending radius), and $\dot{\theta}$ is the speed with which the angular motion is performed.

The division of the continuous time-series data into fixed-size windows is performed by updating the data in the classification window continuously, while the crystal rotates and the signals are acquired from the BLMs. The segmented time-series are normalized and fed into the trained 1D CNN model to predict the class probabilities in real time. At the conclusion of the scan, a feedback mechanism is employed based on the predicted class probabilities to initiate the movement of the crystal to its channeling orientation (which corresponds to the minimum of losses registered at the crystal location during the scan), pending confirmation by the user. This confirmation step by the user serves as a pivotal secondary classification stage conducted by the human operator, given the critical importance of accurately identifying the crystal's channeling orientation. As such, the machine learning algorithm serves as an assistant to the operator, automating the detection of channeling well patterns while awaiting confirmation from the human operator through a double-check process. A flowchart that graphically represents this concept is depicted in Fig. 8. The application with the embedded deep learning model was successfully used in operation with Pb ion beams for the first time in 2022.

Figure 9 depicts the CNN signals during an angular scan. Two distinct BLMS signals, obtained from sensors located in proximity of the crystal and secondary collimator, are fed into the CNN through a translating classification window (depicted as vertical solid lines). The plot shows three output probabilities of the CNN as a function of time during the angular scan. The probability of the analyzed signals representing a channeling well (green line) is initially below 10% during the first half of the scan. However, as the second amorphous plateau is processed by the model and the classification window is updated, the probability of channeling increases and reaches its maximum value. As the scan continues and the pattern of channeling well exits the classification window the no channeling probability rises again.

In Fig. 10, the application of the CNN in another angular scan is depicted. Initially, the probability of a partial well (represented by the black line) is below 10% in the early stages of the scan. However, as the pattern enters in the classification window, the probability of partial well gradually increases, approaching its maximum value. As the scan progresses and the pattern of partial well exits the classification window, the probability of no channeling rises again.

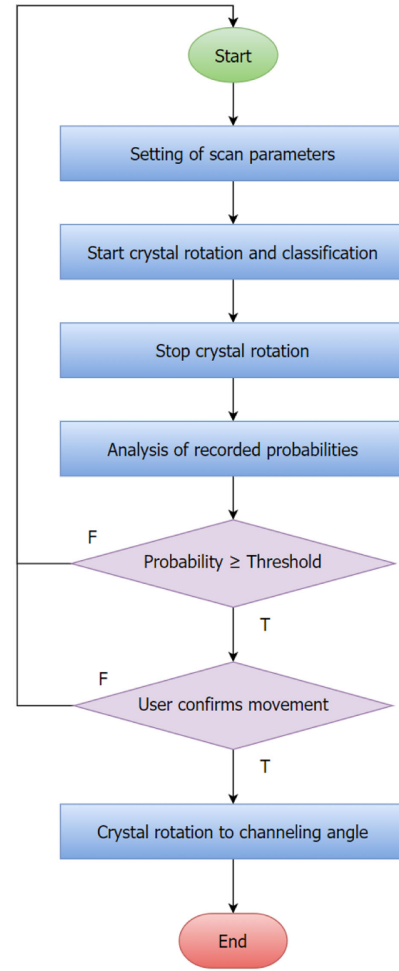


FIG. 8. Flowchart that represents the CNN in use.

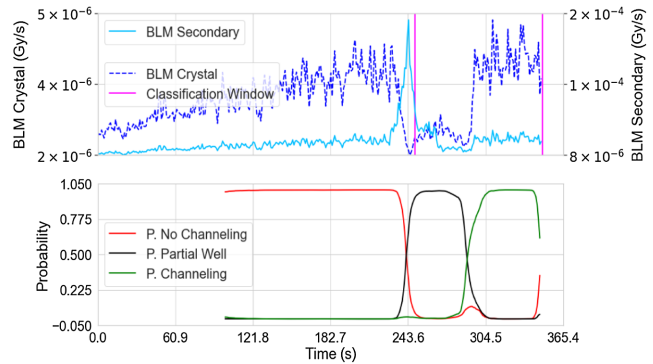


FIG. 9. Top: time-series of BLM signals recorded at the crystal and secondary collimator positions, indicating a channeling well, with vertical solid lines marking the classification window. The input signals for the machine learning model are continually updated as the crystal rotates, causing the classification window to shift over time. Bottom: output probabilities generated by the CNN as a function of time. The CNN output follows the conclusion of the classification window (marked by the right vertical solid line).

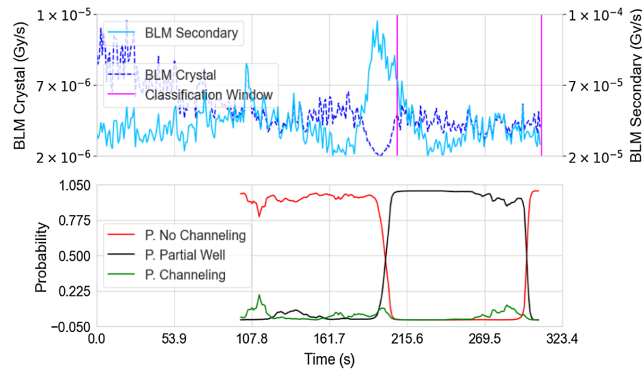


FIG. 10. Top: time-series of BLM signals recorded at the crystal and secondary collimator positions, indicating a channeling well, with vertical solid lines marking the classification window. The input signals for the machine learning model are continually updated as the crystal rotates, causing the classification window to shift over time. Bottom: output probabilities generated by the CNN as a function of time. The CNN output follows the conclusion of the classification window (marked by the right vertical solid line).

VIII. CONCLUSIONS

This study explores the feasibility of using machine learning to automate the process of identifying the main planar channeling conditions of crystal collimators during angular scans. Operational efficiency is crucial for the HL-LHC, and therefore, this work represents a significant step toward automating the angular scans of crystals, which could have a substantial impact on the setup efficiency of future particle accelerators. By integrating machine learning tools into machine operations, our aim is to advance particle accelerator technology, particularly by streamlining the collimator setup process at the LHC. This approach leverages AI-driven tools to enhance automation and improve performance in particle technology, thereby pushing the boundaries of accelerator capabilities.

In this work, the application of a 1D CNN to automatize the process of finding main planar channeling conditions of crystal collimators during an angular scan was studied. The developed model achieved a precision of 93% on unseen validation sets of beam loss monitor signals, confirming the reliability of convolutional networks in classifying time series. Furthermore, a continuous classification scheme has been engineered to integrate the model into an operational tool deployed to effectively achieve its intended purpose online, simplifying the operator task.

This work provides a solid background to future improvements, which will aim at implementing the classification of higher frequency BLM signals. This will potentially provide a 25 Hz online feedback, as opposed to the present 1 Hz, thus allowing the identification of the channeling signature during fast rotations of the crystal, further reducing the time needed for angular scans. This can prove particularly useful in the absence of a previous

reference of the optimal channeling angle (i.e., after a new installation of the crystal), where a large scan of the available rotational range is required.

- [1] O. S. Brüning, P. Collier, P. Lebrun, S. Myers, R. Ostojic, J. Poole, and P. Proudlock, LHC Design Report, CERN Yellow Reports No. CERN-2004-003-V-1: Monographs, CERN, Geneva, 2004, [10.5170/CERN-2004-003-V-1](https://arxiv.org/abs/10.5170/CERN-2004-003-V-1).
- [2] S. Redaelli, Beam cleaning and collimation systems, in *Proceedings of the 2014 Joint International Accelerator School: Beam Loss and Accelerator Protection, Newport Beach, CA* (CERN, Geneva, Switzerland, 2016).
- [3] I. Béjar Alonso, O. Brüning, P. Fessia, M. Lamont, L. Rossi, L. Tavian, and M. Zerlauth, High-Luminosity Large Hadron Collider (HL-LHC): Technical design report, CERN Yellow Reports: Monographs, CERN, Geneva, 2020, [10.23731/CYRM-2020-0010](https://arxiv.org/abs/10.23731/CYRM-2020-0010).
- [4] O. Brüning and L. Rossi, The High-Luminosity Large Hadron Collider, *Nat. Rev. Phys.*, **1**, 241 (2019).
- [5] S. Redaelli, R. Bruce, A. Lechner, and A. Mereghetti, Chapter 5: Collimation system, 2020, pp. 87–114, [10.23731/CYRM-2020-0010.87](https://arxiv.org/abs/10.23731/CYRM-2020-0010.87).
- [6] J. Lindhard, Influence of crystal lattice on motion of energetic charged particles, *Mat. Fys. Medd. K. Dan. Vidensk. Selsk* **34**, 14 (1965), <https://books.google.ch/books?id=b5-LtgAACAAJ>.
- [7] V. M. Biryukov, Y. A. Chesnokov, and V. I. Kotov, *Crystal Channeling and Its Application at High-Energy Accelerators*, 1st ed. (Springer, Berlin, Heidelberg, 2013).
- [8] C. Bahamonde, A. Lechner, and R. Rossi, Crystal channeling of ions on different TCSG materials, in presented at LHC Collimation Upgrade Specification Meeting (CERN, Geneva, 2018).
- [9] H. Belyadi and A. Haghighat, Chapter 5: Supervised learning, in *Machine Learning Guide for Oil and Gas Using Python*, edited by H. Belyadi and A. Haghighat, (Gulf Professional Publishing, 2021), pp. 169–295, [10.1016/B978-0-12-821929-4.00004-4](https://doi.org/10.1016/B978-0-12-821929-4.00004-4).
- [10] S. Redaelli, Beam cleaning and collimation systems, CERN Yellow Reports, Vol. 2 (2016): Proceedings of the 2014 Joint International Accelerator School: Beam Loss and Accelerator Protection, 2016.
- [11] R. W. Assmann, O. Aberle, G. Bellodi, A. Bertarelli, C. Bracco, H. Braun, M. Brugger, S. Calatroni, R. Chamizo, A. Dalocchio, B. Dehning, A. Ferrari, P. Gander *et al.*, The final collimation system for the LHC, in *Proceedings of 10th European Particle Accelerator Conference, EPAC-2006, Edinburgh, Scotland* (EPS-AG, Edinburgh, Scotland, 2006).
- [12] N. Fuster-Martinez, R. Bruce, F. Cerutti, R. D. Maria, P. Hermes, A. Lechner, A. Mereghetti, J. Molson, S. Redaelli, E. Skordis, A. Abramov, and L. Nevay, Simulations of heavy-ion halo collimation at the CERN large hadron collider: Benchmark with measurements and cleaning performance evaluation, *Phys. Rev. Accel. Beams* **23**, 111002 (2020).

- [13] P. D. Hermes, Heavy-ion collimation at the Large Hadron Collider: Simulations and measurements, Ph.D. thesis, Munster U., 2016, <https://cds.cern.ch/record/2241364>.
- [14] N. Fuster Martinez, A. Abramov, G. Azzopardi, E. Belli, C. Boscolo-Meneguolo, R. Bruce, M. D'Andrea, M. Di Castro, M. Fiascari, A. Fomin, H. Garcia-Morales, A. Gorzawski, P. D. Hermes, R. Kwee-Hinzmann, D. Kodjaandreev, A. Mereghetti, D. Mirarchi *et al.*, Run 2 collimation overview, in *Proceedings of the 9th Evian Workshop on LHC Beam Operations, Evian Les Bains, France* (2019), pp. 149–164, <https://cds.cern.ch/record/2750291>.
- [15] W. Scandale, G. Arduini, R. Assmann, C. Bracco, M. Butcher, F. Cerutti, M. D'Andrea, L. S. Esposito, M. Garattini, S. Gilardoni, E. Laface, L. Lari, R. Losito, A. Masi, E. Metral, D. Mirarchi *et al.*, Feasibility of crystal-assisted collimation in the CERN accelerator complex, *Int. J. Mod. Phys. A* **37**, 5 (2022).
- [16] S. Redaelli, M. Butcher, C. Barreto, R. Losito, A. Masi, D. Mirarchi, S. Montesano, R. Rossi, W. Scandale, P. S. Galvez, G. Valentino, and F. Galluccio, First observation of ion beam channeling in bent crystals at multi-TeV energies, *Euro. Phys. J. C* **81**, 142 (2021).
- [17] M. D'Andrea, Applications of crystal collimation to the CERN Large Hadron Collider (LHC) and its High Luminosity Upgrade Project (HL-LHC), Ph.D. thesis, Padua U., 2021, <https://cds.cern.ch/record/2758839>.
- [18] R. Rossi, S. Redaelli, and W. Scandale, Experimental assessment of crystal collimation at the large hadron collider, Ph.D. thesis, Università 'La Sapienza' di Roma, 2017.
- [19] A. A. Garcia, B. Dehning, G. Ferioli, and E. Gschwendtner, LHC beam loss monitors, in *Proceedings of the 5th European Workshop on Diagnostics and Beam Instrumentation, DIPAC-2001, Grenoble, France* (2001), pp. 198–200, <https://cds.cern.ch/record/509291>.
- [20] B. Dehning, E. Effinger, J. Emery, G. Ferioli, G. Guaglio, E. B. Holzer, D. Kramer, L. Ponce, V. Prieto, M. Stockner, and C. Zamantzas, The LHC beam loss measurement system, in *Proceedings of the 22nd Particle Accelerator Conference, PAC-2007, Albuquerque, NM* (IEEE, New York, 2007), pp. 4192–4194.
- [21] M. Butcher, A. Giustiniani, R. Losito, and A. Masi, Controller design and verification for a rotational piezo-based actuator for accurate positioning applications in noisy environments, in *Proceedings of the 41st Annual Conference of the IEEE Industrial Electronics Society, IECON 2015, Yokohama, Japan* (IEEE, New York, 2015), pp. 003887–003892.
- [22] M. D'Andrea, G. Azzopardi, M. D. Castro, E. Matheson, D. Mirarchi, S. Redaelli, G. Ricci, and G. Valentino, Prospects to apply machine learning to optimize the operation of the crystal collimation system at the LHC, in *Proceedings of the 13th International Particle Accelerator Conference, IPAC 2022, Bangkok, Thailand* (JACoW, Geneva, Switzerland, 2022), pp. 1362–1365.
- [23] J. Wagner, R. Bruce, H. Garcia Morales, W. Hofle, G. Kotzian, R. Kwee-Hinzmann, A. S. Langner, A. Mereghetti, E. Quaranta, S. Redaelli, A. Rossi, B. M. Salvachua Ferrando, R. Tomas Garcia, D. Valuch, G. Valentino, and G. Stancari, Active halo control through narrow-band excitation with the ADT, 2016, <https://cds.cern.ch/record/2121286>.
- [24] S. Kiranyaz, O. Avci, O. Abdeljaber, T. Ince, M. Gabbouj, and D. J. Inman, 1D convolutional neural networks and applications: A survey, *Mech. Sys. Signal Process.* **151**, 107398 (2021).
- [25] C. Obermair, T. Cartier-Michaud, A. Apollonio, W. Millar, L. Felsberger, L. Fischl, H. S. Bovbjerg, D. Wollmann, W. Wuensch, N. Catalan-Lasheras, M. Boronat, F. Pernkopf, and G. Burt, Explainable machine learning for breakdown prediction in high gradient rf cavities, *Phys. Rev. Accel. Beams* **25**, 104601 (2022).
- [26] C. Tennant, A. Carpenter, T. Powers, A. Shabalina Solopova, L. Vidyaratne, and K. Iftekharuddin, Superconducting radio-frequency cavity fault classification using machine learning at jefferson laboratory, *Phys. Rev. Accel. Beams* **23**, 114601 (2020).
- [27] F. Chollet, GITHUB—keras-team/keras: Deep learning for humans. <https://github.com/keras-team/keras> [accessed on March 5, 2021].
- [28] M. Abadi *et al.*, TensorFlow: A system for large-scale machine learning, in *Proceedings of the 12th USENIX Conference on Operating Systems Design and Implementation, OSDI-2016, Berkeley, CA* (USENIX Association, USA, 2016), pp. 265–283, ISBN 9781931971331.
- [29] Normalization—machine learning—google developers, <https://developers.google.com/machine-learning/data-prep/transform/normalization?hl=en> [accessed on March 20, 2021].
- [30] L. Prechelt, *Early Stopping—But When?* (Springer, Berlin, Heidelberg, 2012), pp. 53–67.
- [31] J. Bergstra and Y. Bengio, Random search for hyperparameter optimization, *J. Mach. Learn. Res.* **13**, 281 (2012).
- [32] D. Mirarchi, O. Andreassen, R. Bruce, R. Cai, M. D. Castro, M. D'Andrea, M. Hostettler, D. Jacquet, A. Masi, E. Matheson, S. Redaelli, G. Ricci, M. Solfaroli, S. Solis, J. Tagg, and J. Wenninger, Operational handling of crystal collimation at the LHC, in *Proceedings of the 14th International Particle Accelerator Conference, IPAC-2023, Venice, Italy* (JACoW, Geneva, Switzerland, 2023).